

## Magnetic behavior of dilute Rh impurities in $\text{Au}_{1-x}\text{Fe}_x$ alloys: A perturbed-angular-correlation study

V. V. Krishnamurthy, S. N. Mishra, M. R. Press, S. H. Devare, and H. G. Devare

*Tata Institute of Fundamental Research, Homi Bhabha Road, Bombay 400005, India*

(Received 6 May 1994)

We have studied the local magnetic behavior of isolated Rh impurities in  $\text{Au}_{1-x}\text{Fe}_x$  alloys for compositions  $x=0.01, 0.03, 0.10,$  and  $0.18,$  using the time-differential perturbed-angular-correlation (TDPAC) method and by electronic structure calculations within the local spin-density (LSD) approximation. From the measured Curie-Weiss local susceptibility of the  $^{100}\text{Rh}$  probe as well as the LSD calculations we find large stable magnetic moments  $0.5-1.0\mu_B$  on Rh for compositions  $x \geq 0.10.$  In low Fe concentration alloys the observed weak local susceptibility can be reconciled with the calculated large local moments, both positive and negative, on Rh in terms of a typical Ruderman-Kittel-Kasuya-Yosida (RKKY)-type mechanism between Fe and Rh. In the reentrant spin-glass regime,  $T \leq 60$  K for  $x=0.18,$  the hyperfine field  $B_{\text{hf}}$  shows a two-step temperature dependence, increasing sharply below 60 K, such that its extrapolated value at 0 K is enhanced by 30% over its saturated value in the ferromagnetic region.

### I. INTRODUCTION

The problem of magnetic moment formation on isolated  $4d$  ions in a variety of metal hosts, such as spin glasses, transition-metal hosts, monolayers, overlayers, and clusters, is attaining growing interest as revealed by the increasing number of experimental as well as theoretical papers.<sup>1-3</sup> Recently, Gross and co-workers<sup>1</sup> have found spin magnetic moments with large spin-fluctuation temperatures for Ru and Rh impurities in a Pd host. Stable magnetic moments at Rh in dilute Pd-Fe alloys were also reported,<sup>4</sup> and confirmed by local spin-density calculations.<sup>5</sup> Rh was found to have nearly stable magnetic moment in exchange enhanced Ni-Rh alloys when surrounded by at least six Ni atoms in the first-nearest-neighbor (1nn) shell surrounding the central Rh atom.<sup>6</sup> All these results indicate a magnetic moment of up to  $1.0\mu_B$  on Rh. In general, the stability of  $4d$  magnetic moment in these systems is found to be strongly correlated with the magnetic environment and the strength of the interatomic ferromagnetic interaction.

In a theoretical calculation, Willenborg, Zeller, and Dederichs<sup>7</sup> have predicted Mo and Tc impurities to be magnetic in the noble-metal hosts Ag and Au. However, using the perturbed-angular-distribution (PAD) technique, Riegel *et al.*<sup>8</sup> found that Mo is nonmagnetic in both the hosts. This discrepancy was attributed to the dynamic correlations between conduction electrons and a local moment which cannot be treated within the one-electron theory of Ref. 7. Recently, Zhu, Bylander, and Kleinman<sup>9</sup> calculated large magnetic moment of  $1.09\mu_B$  on Rh for a Rh monolayer on a Au(001) surface; this indicates that the Rh atoms, at least in reduced dimensions, acquire a magnetic moment in Au. On the other hand, isolated Rh impurity in bulk Au metal has been found to be nonmagnetic.<sup>10</sup> In view of these contrasting results, it is of interest to investigate under what conditions a local

magnetic moment appears on a  $4d$  impurity like Rh when embedded in a noble-metal host, e.g., Au. In this direction we have investigated the magnetic behavior of isolated Rh impurities in  $\text{Au}_{1-x}\text{Fe}_x$  alloys using the time-differential perturbed-angular-correlation (TDPAC) method, mainly to study the influence of a strongly magnetic neighboring atom, such as, Fe, on the magnetism of Rh. Alongside, we have also performed electronic structure calculations using the local spin-density (LSD) approximation to support our experimental results and conclusions drawn regarding the local magnetism of Rh in these alloy systems.

Among the well documented exotic characteristics of  $\text{Au}_{1-x}\text{Fe}_x$  alloys is the reentrant spin-glass (RSG) behavior for  $0.15 < x < 0.25,$  which is characterized by two successive magnetic transitions, namely, paramagnetic to ferromagnetic at  $T_c$  and followed by a transition to the spin-glass state below  $T_g.$  Microscopic studies on the reentrant magnetic behavior in Au-Fe alloys have been made<sup>11-13</sup> using Mössbauer spectroscopy of  $^{57}\text{Fe},$   $^{119}\text{Sn},$  and  $^{197}\text{Au},$  as well as by the TDPAC method with  $^{111}\text{Cd}$  probe.<sup>14</sup> However, the analysis of these data suffer from the inherent (complications arising from) difficulties in resolving magnetic and quadrupole interaction strengths present in these disordered alloys. The  $^{100}\text{Rh}$  probe, with large  $g_N=2.15$  and very small nuclear quadrupole moment of  $0.08b,$  in combination with the TDPAC technique is ideal for the study of the magnetic transitions, in particular the reentrant magnetic behavior, in Au-Fe alloys. Further, the TDPAC method allows for the measurement of the hyperfine fields and nuclear-spin-relaxation rates at any temperature, which lead to the determination of spin polarization, local magnetic moments, and spin-fluctuation temperatures.

In this paper we present our results on the magnetic behavior of isolated Rh impurities in some  $\text{Au}_{1-x}\text{Fe}_x$  alloys with  $x$  varying from 0.01 to 0.18, studied via the

TDPAC technique following recoil implantation. The experimental results are augmented with illustrative local spin-density calculations performed using the linear combination of atomic orbitals-molecular orbitals (LCAO-MO) method to estimate the spin magnetic moments at Fe and Rh atoms for a few interesting cases of neighboring Au and Fe atom coordinations. From the measured Curie-Weiss local susceptibility at  $^{100}\text{Rh}$  probe as well as LSD calculations we find sizable and stable local magnetic moments at Rh of up to  $\sim 1.0\mu_B$  in magnitude for compositions  $x \geq 0.10$ . In very low Fe concentration alloys  $x \leq 0.03$  the observed weak local susceptibility can be reconciled with the significant calculated local moments, both positive and negative, on Rh in terms of a Ruderman-Kittel-Kasaya-Yasuda (RKKY)-type indirect exchange mechanism between Fe and Rh. The reentrant spin-glass regime of the  $x=0.18$  alloy is signaled by a kink and a sharp increase in the hyperfine field at Rh below  $T_g=60$  K, such that its extrapolated value at 0 K is enhanced by 30% over its saturated value in the ferromagnetic region.

In Sec. II we outline the experimental techniques and report the results; electronic structure calculations are presented in Sec. III; this is followed in Sec. IV by a discussion of the results and concluding remarks.

## II. EXPERIMENT

### A. Experimental method

$\text{Au}_{1-x}\text{Fe}_x$  alloys with  $x=0.01, 0.03, 0.10,$  and  $0.18$  were prepared by arc-melting stoichiometric compositions of high-purity elements Au and Fe in argon atmosphere. The alloys were annealed at  $750^\circ\text{C}$  for 22 h and quenched to room temperature. The compositions of individual elements in the alloys were verified by the electron microprobe analysis and energy-dispersive analysis of x rays.

The parent  $^{100}\text{Pd}$  activity was produced and recoil implanted into thin (typically  $5 \text{ mg/cm}^2$ ) foils of Au-Fe alloys using the heavy-ion reaction  $^{89}\text{Y}(^{16}\text{O}, p4n)$  with a 95-MeV  $^{16}\text{O}$  beam, provided by the Pelletron accelerator at TIFR, Bombay. By the application of TDPAC method, the magnetic interaction was detected using the  $74 \text{ keV}, I^\pi=2^+$  level in  $^{100}\text{Rh}$  with  $T_{1/2}=235 \text{ ns}$  and  $g_N=2.15$ , populated by the electron-capture decay of  $^{100}\text{Pd}$ . The concentration of the implanted  $^{100}\text{Rh}$  in Au-Fe alloys was typically less than 1 ppm. The measurements were carried out for temperatures between 20 and 700 K in an external magnetic field of 11 kG. The PAC time spectra were recorded using three NaI(Tl) detectors in  $0, \pm 135^\circ$  geometry and a standard coincidence circuit. From the normalized coincidence counts,  $N(\pm 135^\circ, t)$ , of each detector the ratio functions<sup>13</sup>

$$R(t) = [N(135^\circ, t) - N(-135^\circ, t)] / [N(135^\circ, t) + N(-135^\circ, t)] \quad (1)$$

were generated and fitted by the function

$$R(t) = (3/4)A_2 e^{-\lambda t} \sin(2\omega_L t - \phi) \quad (2)$$

to extract the Larmor frequency  $\omega_L$ , from which the effective magnetic field acting at the nucleus  $B_{\text{eff}} = B_{\text{ext}} + B_{\text{hf}}$  can be obtained via the relation  $\omega_L = \hbar^{-1} g_N \mu_N B_{\text{eff}}(T)$ . In the paramagnetic region, the enhancement factor  $\beta(T) = B_{\text{eff}}(T)/B_{\text{ext}}$  yields a measure of the local susceptibility  $\chi_{\text{loc}}(T) \equiv \beta(T) - 1$ . Greater details of the TDPAC method can be found in Ref. 15.

### B. Experimental results

Figures 1(a) and 1(b) show some typical spin-rotation spectra obtained for the different Au-Fe alloys at different temperatures. All the spectra show nearly full anisotropy suggesting that the majority of the recoiling  $^{100}\text{Pd}$  ions come to rest at unique lattice sites in the host. The spectra, particularly of the high-Fe concentration alloys, show significant damping [the exponential factor in Eq. (2)] which can be a consequence of the distribution in the interaction frequencies arising from the different near-neighbor (nn) atomic coordination around the central Rh probe atom as well as time-dependent fluctuations of the magnetic moments. Due to the limited accuracy of our measurements we have not observed distinctly resolved frequencies corresponding to different nn configurations. Thus we extract from the measured spectra only a single Larmor frequency representative of an averaged hyperfine field over all possible nn coordinations.

Figure 2 shows the paramagnetic enhancement factor  $\beta(T)$  as a function of inverse temperature for all alloy compositions. For the dilute alloys,  $x=0.01$  and  $0.03$ ,  $\beta(T)$  is slightly greater than unity with weak temperature dependence. For  $x=0.10$  and  $0.18$ ,  $\beta(T)$  shows strong temperature dependence, which, when parametrized by the Curie law  $\beta-1 \equiv C/T$ , yields Curie constants  $C = -72$  and  $-112 \text{ K}$ , respectively. These large negative  $C$  values are suggestive of the presence of large spin polarization centered around the Rh atom. For completeness, we mention that measurements in quenched and virgin cast samples for  $x=0.10$  and  $0.18$  gave nearly identical values of  $\beta(T)$  (see Fig. 2) suggesting the absence of large scale variation in the atomic environment due to clustering of Fe in our samples.

Figure 3 shows typical  $R(t)$  spectra for the quenched alloy of  $\text{Au}_{0.82}\text{Fe}_{0.18}$  below its ferromagnetic ordering temperature  $T_c \sim 180 \text{ K}$ . The measurements were carried out in external magnetic field of 11 kG. The hyperfine field  $B_{\text{hf}}$  values extracted from these spectra are shown in Fig. 4.

## III. THEORY

To corroborate our experimental findings, we also perform electronic structure calculations on probe Rh in the Au-Fe system using the *ab initio* discrete variational self-consistent-field linear combination of atomic orbitals forming molecular orbitals (LCAO-MO) method<sup>16</sup> within the framework of the local spin-density (LSD) functional formalism<sup>17</sup> and employing an atomic clusters model to simulate the bulk. In brief, 19 atom clusters  $M_1 M_{12} M_6$  ( $M \equiv \text{Au, Fe or Rh}$ ) representing two full coordination

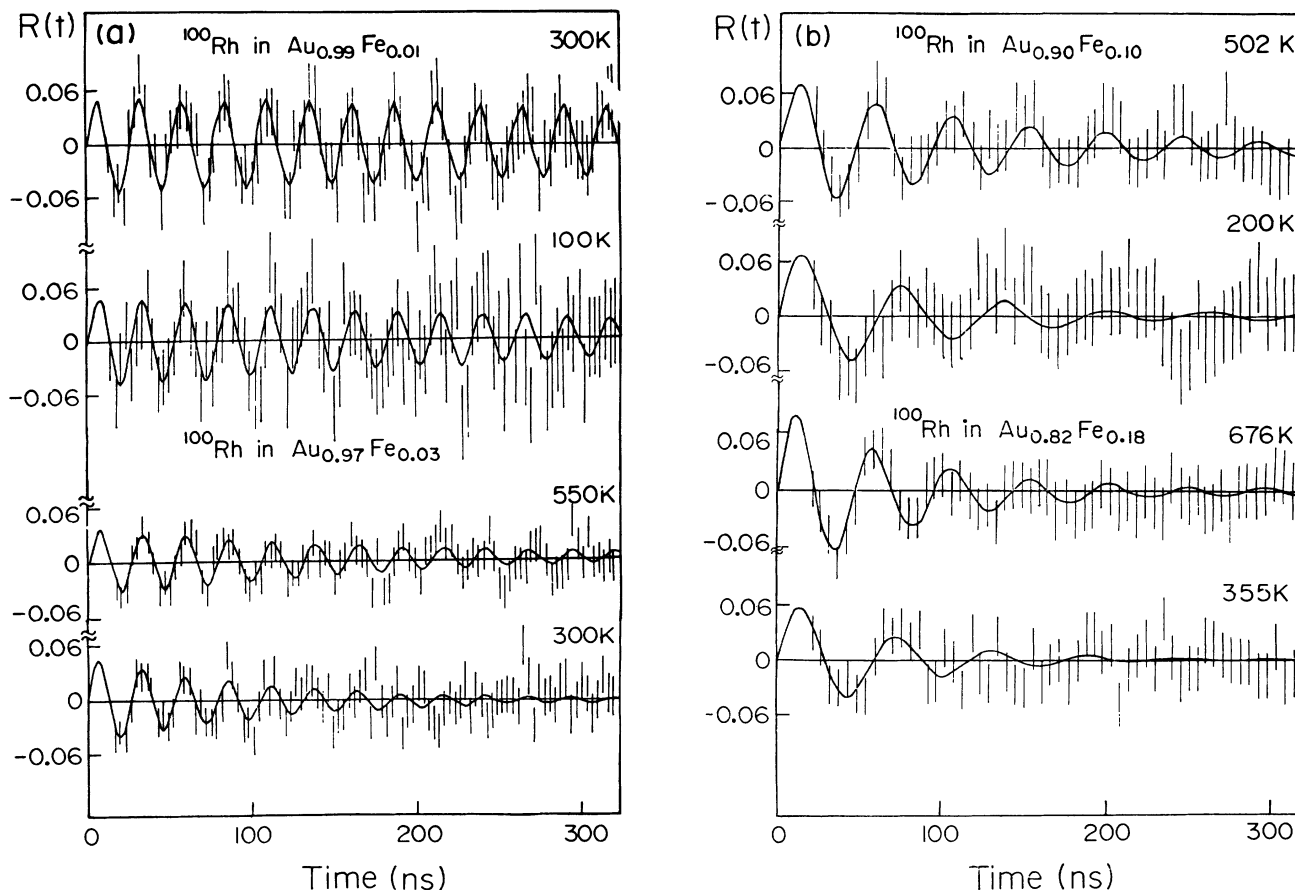


FIG. 1. Spin rotation spectra of  $^{100}\text{Rh}$  in different Au-Fe alloys measured at different temperatures in an external field of 11 kG.

shells of atoms around a central probe atom  $M_1$  in the fcc lattice geometry of Au metal ( $a = 4.08 \text{ \AA}$ ) are chosen for explicit treatment of their eigenfunctions and eigenvalues. The probe Rh atom is always at the  $M_1$  site. In the absence of actual structural models for  $\text{Au}_{1-x}\text{Fe}_x$  alloys

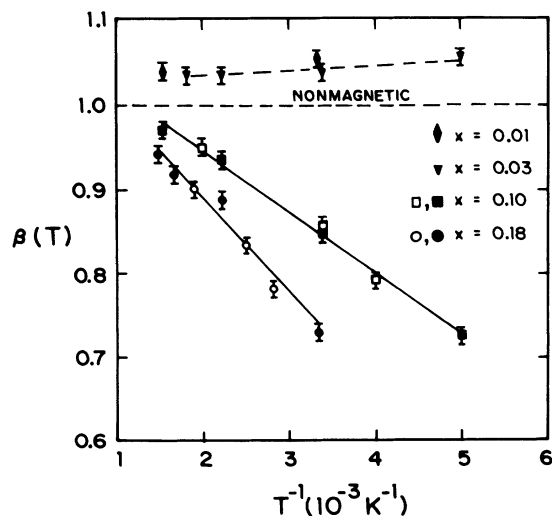


FIG. 2. The paramagnetic enhancement factor  $\beta(T) = B_{\text{eff}}/B_{\text{ext}}$  for different Au-Fe alloys plotted versus the inverse temperature  $T^{-1}$ . Filled and open symbols correspond to the data taken on virgin cast and quenched samples, respectively.

with different Fe concentration  $x$ , we attempt illustrative model calculations in which up to 4 Au atoms are replaced by Fe atoms among the first- and second-neighbor (1nn and 2nn) shells to simulate some local environments in these dilute alloys. The idea is not a comprehensive survey of all possible distributions, but rather to glean the basic result and the interaction mechanism, and see how certain derived quantities (Curie constant  $C$ , local density of states, etc.) compare with their experimentally determined values.

The variational basis set consists of numerical atomic orbitals:  $5d$ ,  $6s$ ,  $6p$  on Au;  $3d$ ,  $4s$ ,  $4p$  on Fe; and  $4d$ ,  $5s$ ,  $5p$  on Rh. The deeper-lying core orbitals are left unchanged but they do contribute to the construction of the potential. The occupation of the atomic valence  $d$  orbitals is reiterated to closely match those obtained for the bulk. The exchange-correlation potential in the single particle LSD equations is of the form given by von Barth and Hedin.<sup>18</sup> The Hamiltonian and overlap matrix elements are constructed by numerical integration over a grid of diophantine sampling points, outside of a systematic polynomial integration around the  $M_1$  site. The Rayleigh-Ritz secular equation is then solved iteratively to self-consistency to obtain the cluster eigenvalues and eigenfunctions. The eigenfunctions are then analyzed by a Mulliken population scheme into atomic orbital occupation numbers and the discrete energy levels are

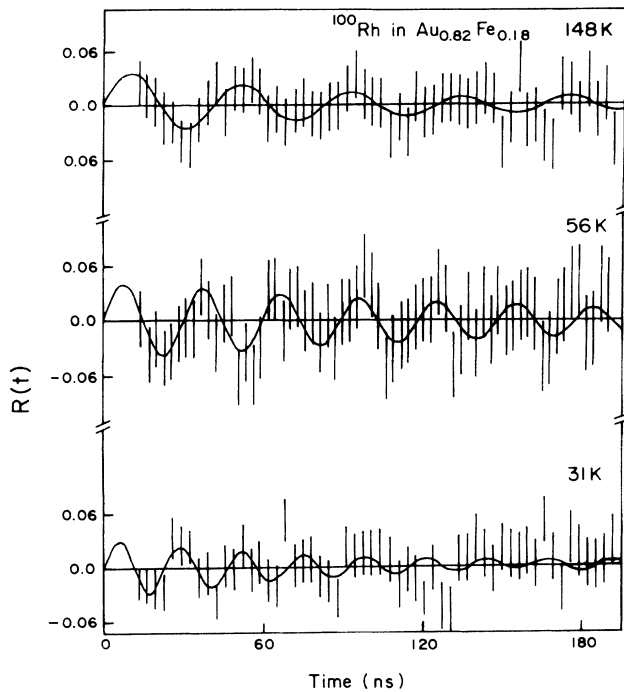


FIG. 3. Spin-rotation spectra of  $^{100}\text{Rh}$  in the ferromagnetic and reentrant spin-glass regions of  $\text{Au}_{0.82}\text{Fe}_{0.18}$  at different temperatures in an external field of 11 kG.

broadened into solid-state bands using<sup>5</sup> a Lorentzian broadening of 0.4 eV. An additional fallout of the calculation is the valence electron contribution to the contact hyperfine field at the  $M_1$  nuclear site, given by  $H_{\text{hf}}^{\text{val}} = 524.2[\rho_{\uparrow}(0) - \rho_{\downarrow}(0)]$  kG, where  $\rho_{\uparrow,\downarrow}(0)$  and the majority and minority electron charge densities at the nucleus, to add to the contribution  $H_{\text{hf}}^{\text{core}}$  from the polarization of the core electrons due to unequal spin-up and spin-down electrons in the transition  $d$  orbital.

The present nonrelativistic treatment of the heavy met-

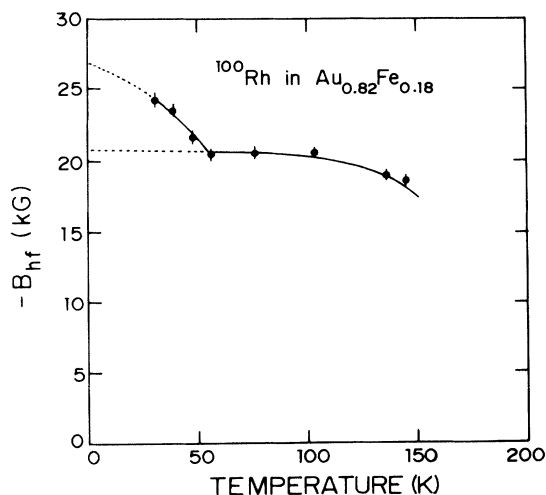


FIG. 4. Temperature variation of the average hyperfine field  $B_{\text{hf}}$  at Rh in  $\text{Au}_{0.82}\text{Fe}_{0.18}$ .

al Au can be justified in the present case by the following considerations. We note that Au is expected to have a low-lying, filled  $5d$  band; the eigenvalue of its atomic  $5d$  level is at least 1.5 eV below both the  $3d$  state of Fe and the  $4d$  of Rh having the self-consistent occupations of the bulk. Rather, it is the  $6s$  atomic level of Au (for which LS coupling is irrelevant) that is within 1 eV of the probe  $d$  levels, so it is hybridization of the probe  $d$  with the host  $sp$  orbitals that is expected to play a dominant role. Further, as to the magnetic aspects, a comparison<sup>19</sup> of the semirelativistic and nonrelativistic calculations of the magnetic moments and hyperfine fields for  $3d$  and  $4d$  impurities in Ni has shown that relativistic effects increase the local  $d$  moments formed only minimally.

Our results from the cluster calculations on the host Au and probe atoms in Au are summarized in Table I; the local density of states (LDOS) for the probe atoms are given in Fig. 5, wherein all energies are relative to the Fermi energy  $E_F$ . A Au atom in bulk Au metal shows a 5-eV broad, fully filled ( $5d^{9.82}$ )  $d$  band with its upper edge 3 eV below  $E_F$ ; bonding, nonbonding, and antibonding orbitals of  $sp$  character are also seen at  $-6$  to  $-7$  eV, at

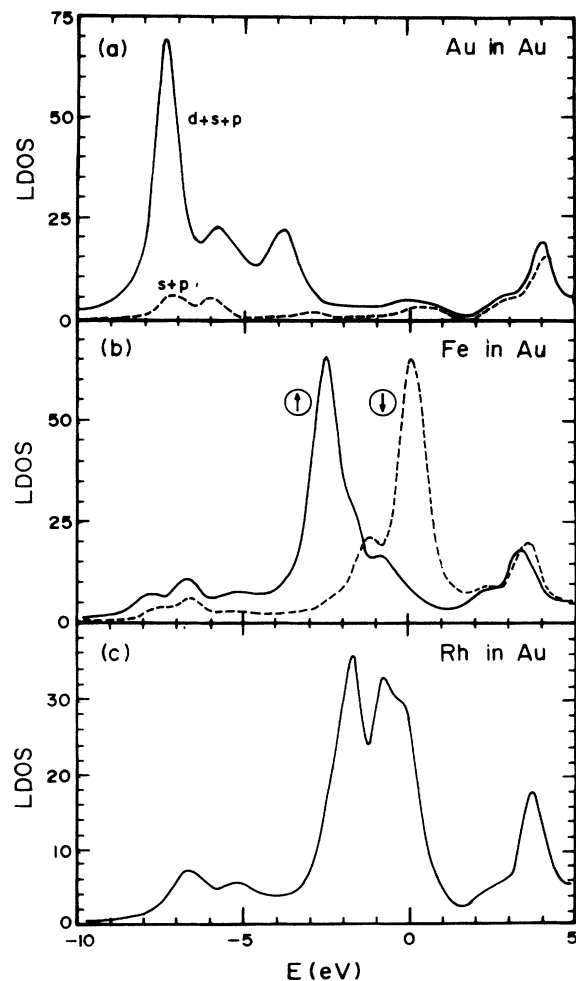


FIG. 5. Local density of states (LDOS) in arbitrary units with energy relative to the Fermi energy for (a) a Au atom, (b) an Fe atom, and (c) a Rh atom, in Au metal.

TABLE I. Summary of parameter values for the Au-Fe system from cluster calculations.  $n_{\uparrow}$  and  $n_{\downarrow}$  are the number of spin-up and spin-down electrons in the  $d$ ,  $s$ , and  $p$  orbitals;  $Q$  is the net ionicity and  $\mu$  is the net local moment;  $N_F$  is the local density of states at the Fermi energy;  $B_{\text{hf}}$  is the calculated hyperfine field with contributions  $H_{\text{hf}}^{\text{core}}$  and  $H_{\text{hf}}^{\text{val}}$  as explained in the text—all for the central probe  $M_1$  atom.  $\mu_{\text{tot}}$  is the net moment on the cluster.

Cluster employed $M_1 M_{12} M_6$	Cluster symm.	Cluster geometry (Å)	$(n_{\uparrow} + n_{\downarrow})(M_1)$			$Q(e^-)$ $\mu(\mu_B)$	$\mu_{\text{tot}}$ $(\mu_B)$	$N_F(M_1)$ sts./eV	$B_{\text{hf}}^{\text{core}} + B_{\text{hf}}^{\text{val}}$ $= B_{\text{hf}}(M_1)$ (kG)
			$d$	$s$	$p$				
Au <sub>1</sub> (Au <sub>12</sub> )Au <sub>6</sub>	$O_h$	$a = 4.08$	9.82	0.48	0.70	0.00	0	0.38	0+0
		$d = 2.88$	0.00	0.00	0.00	0.00			=0
Fe <sub>1</sub> Au <sub>12</sub> Au <sub>6</sub>	$O_h$	$a = 4.08$	6.80	0.49	0.57	+0.14	4	2.62	-295+200
		$d = 2.84$	2.96	0.10	0.15	3.21			= -95
Rh <sub>1</sub> Au <sub>12</sub> Au <sub>6</sub>	$O_h$	$a = 4.08$	8.54	0.18	0.22	+0.06	0	2.06	0+0
		$d = 2.86$	0.00	0.00	0.00	0.00			=0
Rh <sub>1</sub> (Au <sub>4</sub> Au <sub>8</sub> ) (Au <sub>4</sub> Fe <sub>2</sub> )	$D_{4h}$	$a = 4.08$	8.53	0.20	0.36	-0.09	5	1.74	290+50
		$d = 2.86$	-0.83	-0.005	-0.01	-0.845			= +340
Rh <sub>1</sub> (Fe <sub>2</sub> Au <sub>8</sub> Au <sub>2</sub> ) (Au <sub>4</sub> Au <sub>2</sub> )	$D_{2h}$	$a = 4.08$	8.52	0.25	0.40	-0.17	7	1.99	-195+30
		$d = 2.86$	0.56	-0.01	-0.035	0.515			= -165
Rh <sub>1</sub> (Fe <sub>4</sub> Au <sub>8</sub> ) (Au <sub>4</sub> Au <sub>2</sub> )	$D_{4h}$	$a = 4.08$	8.49	0.29	0.38	-0.16	13	1.84	-315+5
		$d = 2.86$	0.90	-0.03	-0.09	0.78			= -310

0 eV, and around +4 eV, respectively. Using a fully relativistic spin-polarized embedded-cluster method also within LSD functional theory, Weinberger *et al.*<sup>20</sup> obtain for Au a 5.5-eV-wide  $d$  band starting at 1.5 eV below  $E_F$ .

Note that when Fe and Rh atoms are at the  $M_1$  site in the clusters, we have relaxed our 1nn distance by 0.04 Å for Fe and by 0.02 Å for Rh to account, in some measure, for the smaller sizes of the substitute atoms. An isolated Fe atom at a substitutional site in Au exhibits a narrow band of majority  $d$ -spin orbitals centered at -2.5 eV, immediately above the host  $d$  band, and minority  $d$ -spin orbitals at  $E_F$ ; the exchange splitting is thus 2.5 eV. The LDOS for a single Fe impurity in Au as obtained in Ref. 15 shows narrow majority and minority peaks of  $d$  character at -1.5 and +0.25 eV, respectively. Thus the placement of our  $d$  bands, both for Au and Fe, is lower by  $\geq 1$  eV. The integrated  $3d$  charge density is closer to  $d^7$  rather than the  $d^5-d^6$  configurations inferred from magnetic-susceptibility measurements<sup>21</sup> on dilute Au-Fe alloys. The integrated spin magnetization density gives a local Fe  $d$  moment of  $2.96\mu_B$ , which compares well with the  $3.12\mu_B$  “ $d$ -like” moment of Ref. 20, and substantial positive polarizations also for the  $4sp$  conduction-band orbitals. Clearly the lower placement of the Au  $d$  band has not affected the DOS structure near  $E_F$  that leads to local moment formation, and gives credence to our results for the magnetism of Rh in Au-Fe to follow. However, the extension of these narrow bands suggests considerable impurity-host  $d$ - $sp$  hybridization.

The  $6sp$  orbitals of the 1nn Au atoms acquire a slight antiferromagnetic polarization, of  $\sim -0.01\mu_B$ , relative to the Fe atom, consistent with the RKKY-type indirect exchange expected in this canonical spin-glass system.<sup>22</sup> (The oscillations in the local moment at the Au sites show up better for cluster calculations of the type shown in rows 4 and 5 of Table I, but with a Au atom at the central  $M_1$  site.) However, it must be conceded that even these small moments are overestimated in magnitude due

to the spurious effect of being on extended orbitals on atoms on the surface of the cluster which do not have the full complement of coordinating atoms; this effect is even more drastic for the Au<sub>6</sub> atoms. In a larger cluster this adjustment would be shunted out to the outermost atoms thereby giving a larger volume of the bulk with authentic moments. Taking only the inner Fe<sub>1</sub>+Au<sub>12</sub> atoms, the net moment obtained is  $\mu_{\text{tot}} \sim 3\mu_B$ , whereas the outermost Au<sub>6</sub> shell adjusts to give a net cluster moment of  $4\mu_B$ , an even integer value determined by the fact that the Fe atom has an even number of electrons. This spurious surface polarization accounts also for the exaggerated value of +200 kG calculated for the transferred valence hyperfine field at Fe, when compared with the value of +100 kG extracted from a net hyperfine field of -200 kG, determined from Mössbauer spectroscopy<sup>23</sup> and using  $B_{\text{hf}}^{\text{core}} = -100 \text{ kG}/\mu_B$  for the core- $d$  hyperfine field of Fe.<sup>19</sup> Using this experimental value of -200 kG for  $B_{\text{hf}}$  and  $\mu_{\text{tot}} = 3\mu_B$  (or  $S_i = 1.5$ ) per Fe atom in the expression for the Curie constant  $C = g_S \mu_B (S_i + 1) B_{\text{hf}} / 3k_B$ , yields

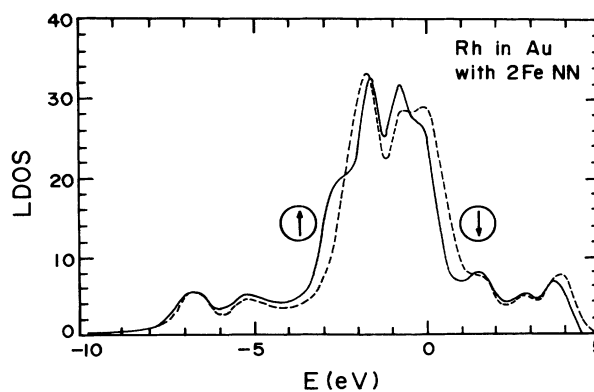


FIG. 6. Local density of states (LDOS) in arbitrary units with energy relative to the Fermi energy for a Rh atom in Au metal with two nearest-neighbor Fe atoms.

$C = -22$  K, consistent with the value  $-25$  K obtained using the TDPAD method.<sup>24</sup>

An isolated substitutional Rh atom in a host Au matrix is seen to be nonmagnetic. The LDOS for Rh shows a broad  $d$  band, 3 eV wide, again from just above the Au  $d$  band and extending up to  $E_F$ , with  $t_{2g} - e_g$  splitting of 1.25 eV; again there is noticeable impurity-host  $d-d$  hybridization in the valence region and  $d-sp$  overlap in the conduction band. The 8.54 electron count in the  $4d$  orbital of Rh appears to be a compromise between the experimental  $4d^8 5s^1$  atomic ground state and the  $4d^9$  ground state obtained using LSD.

The above results are preparatory reference for our main result to follow. That is, a Rh atom in Au metal when surrounded by two to four Fe atoms in 1nn is seen to develop significant local  $d$  moments between  $0.5$  and  $1.0\mu_B$  in response; not surprisingly, with 2nn Fe atoms, the Rh  $d$  moment is also substantial but aligned antiferromagnetically with respect to the Fe moment. These values for  $\mu(\text{Rh})$  are in the same range as for local moments stabilized on Rh atoms in dilute Pd-Fe alloys<sup>5</sup> and in Ni-Rh alloys,<sup>6</sup> and in small clusters of Rh,<sup>3</sup> no local moments on Rh larger than  $1\mu_B$  have been observed. This suggests that the Rh moment saturates very quickly in the neighboring presence of a few (say  $\gtrsim 2$ ) Fe atoms. The net cluster moment is almost entirely accounted for by the  $\sim 3\mu_B$  per Fe atom plus the Rh moment. At least within the cluster size, the Au atoms acquire an antiferromagnetic polarization which, though still very small, on the average exceeds that for the case of a single Fe atom in Au case.

The LDOS for a Rh probe having two 1nn Fe atoms is shown in Fig. 6. The main differences from Fig. 5(c) are the onset of a shoulder at  $-2.5$  eV due to Fe-Rh  $d-d$  interaction, and the development of an exchange splitting which creates a virtual bound state (essentially, the difference between the two spin LDOS) with a signature double hump straddling  $E_F$ . Also, the  $d-sp$  hybridization peak 3–4 eV above  $E_F$  for Rh in Au is smeared into a more uniform increase in LDOS above  $E_F$ . Clearly, the presence of Fe provides a ready-made band of minority spin states just above  $E_F$  which is now preferentially occupied by the Rh  $d$  electrons and leads to the observed exchange splitting at the Rh site. In all cases, there is minimal charge transfer between the probe Rh and the host atoms, and no perceptible change in the occupation of the Rh  $4d$  orbitals either.

#### IV. DISCUSSION

We first discuss the magnetic behavior of Rh in the paramagnetic region of  $\text{Au}_{1-x}\text{Fe}_x$  alloys. As mentioned above, the observed Rh local susceptibility in the alloys with  $x = 0.1$  and  $0.18$  show strong temperature dependence (see Fig. 2). The total paramagnetic local susceptibility  $\chi_{\text{loc}} \equiv \beta(T) - 1$  at a probe site can be written as

$$\chi_{\text{loc}}(T) = \chi_{\text{loc}}^p + \chi_{\text{loc}}^s(T) + \chi_{\text{loc}}^d(T), \quad (3)$$

where  $\chi_{\text{loc}}^p$  is the temperature-independent contribution to  $\chi_{\text{loc}}$  from the Pauli spin susceptibility of the host

conduction-band electrons and  $\chi_{\text{loc}}^s(T) = \chi_{\text{loc}}^{\text{self}}(T) + \chi_{\text{loc}}^{\text{tr}}(T)$  is the temperature-dependent contribution arising from the self-polarization of the valence electrons of the probe [ $\chi_{\text{loc}}^{\text{self}}(T)$ ], by the localized magnetic moments at the probe if any and from the transferred hyperfine field produced by the magnetic environment ( $\chi_{\text{loc}}^{\text{tr}}$ ). The last term  $\chi_{\text{loc}}^d(T)$  corresponds to the contribution arising from the core polarization due to the spin imbalance in the probe  $d$  orbitals. Assuming that Rh atoms have no  $d$  moment, the temperature dependence of  $\chi_{\text{loc}}$  would arise mainly from  $\chi_{\text{loc}}^{\text{tr}}$ , which is proportional to the Fe moment. An estimation of  $\chi_{\text{loc}}^{\text{tr}}$  can be made using the relation<sup>27</sup>

$$\chi_{\text{loc}}^{\text{tr}} = 2[(g_J - 1)/g_J] B_{\text{tr}} \chi(T) / (N\mu_B),$$

where  $B_{\text{tr}}$  is the transferred hyperfine field per unit local moment,  $\chi(T)$  is the bulk susceptibility of the host. The  $B_{\text{tr}}$  values for  $4d$  impurities in the Fe host has been estimated to be<sup>28,29</sup>  $\sim -130$  kG/ $\mu_B$ . Using this value for  $B_{\text{tr}}$  and our high-temperature bulk susceptibility data measured for  $x = 0.18$  we estimate the upper limit of the contribution from  $B_{\text{tr}}$  to the local Curie constant as  $-15$  K, which is far smaller in magnitude than the observed value of  $-112$  K. For  $x = 0.10$ , the corresponding contribution is also small,  $-8$  K. This clearly implies that majority contribution to the local susceptibility arises from the core polarization of the Rh  $d$  orbitals suggesting a local magnetic moment thereon.

As mentioned above our LSD calculation shows substantially large local magnetic moment on Rh when surrounded by two or more Fe atoms in the neighboring shells. The magnetic moment at Rh site comes out to be in the range of  $0.5-0.8\mu_B$  for two and four Fe atoms in the 1nn shell. On the other hand, for Fe atoms placed in the 2nn shell also, Rh acquires a large spin polarization corresponding to a magnetic moment of  $\sim 0.85\mu_B$  which is now antiferromagnetically aligned with respect to the moment at the Fe site. The decoration of Fe atoms considered in our cluster calculations becomes statistically relevant for concentrations  $x \gtrsim 0.1$ . Due to the reduced symmetry ( $C_1$ ), we are unable to study the response of a Rh atom in the vicinity of a single 1nn or 2nn Fe atom. But considering the symmetrical positions of the Fe atoms around Rh, for which one expects the polarization effects of each Fe neighbor on Rh to add up coherently, one may infer from our results that, for the case of one Fe atom nearby the Rh atom, (a) the magnetic moment on Rh will persist, though of reduced strengths in individual cases, and (b) the above trend in the sign of the Rh magnetic moments relative to Fe would still hold. Thus, though our cluster calculations are few and illustrative, they are adequate to show that Rh atoms in Au-Fe alloys will always exhibit some stable local moments even in the presence of one Fe atom. The inferred oscillatory behavior of Rh moment is consistent with a standard RKKY mechanism where the  $sp$  band of the Au matrix mediates the indirect exchange interaction.

Using the binomial expansion and a simplified scenario with  $\mu(\text{Fe}) = 3\mu_B$ ,  $\mu(\text{Rh})_{\text{av}} = 1\mu_B$ , and  $\mu(\text{Au}) = 0\mu_B$ , as typical local moment values across the board for all configurations (except the manifestly nonmagnetic ones)

along with a Rh-Fe ferromagnetic coupling, we obtain estimates for the Curie constant as  $C = -65$  K for  $x = 0.10$  and  $C = -92$  K for  $x = 0.18$ , in fair agreement with the  $C$  values  $-72$  and  $-112$  K extracted in Sec. II. Extending the expansion out to further shells of atoms would certainly better the agreement.

The total spin polarization and hence the magnetic moment at Rh in  $\text{Au}_{1-x}\text{Fe}_x$  alloys with  $x = 0.10$  and  $0.18$  can be estimated from the Curie constants derived from the experimentally observed paramagnetic local susceptibility  $\beta(T) - 1$  data using the relation<sup>15</sup>  $C = 2\mu_B(S_t + 1)B_{\text{hf}}(0)/3k_B$ . Here  $B_{\text{hf}}(0)$  is the zero-temperature contact hyperfine field at the Rh nucleus,  $S_t = S_{\text{probe}} + S_{\text{host}}$  is the sum of the spin polarization at the probe atom and the spin polarization on the host near-neighbor atoms. For most  $4d$  ions  $B_{\text{hf}}(0)$  have been found to be  $-350$  kG/ $\mu_B$ .<sup>25</sup> For a consistent explanation of our experimental results with the LSD calculated magnetic moment at Rh we have used  $B(0) = -350$  kG to extract the total spin polarization  $S_t$  and the total moment  $\mu_{\text{tot}}$  seen by Rh which come out to be  $3.63$ ,  $7.26\mu_B$  and  $6.2$ ,  $12.4\mu_B$  for  $x = 0.10$  and  $0.18$ , respectively. The high value of the total magnetic moment  $\mu_{\text{tot}}$  agrees well with the estimated net magnetic moment over the closest 18 atoms around Rh (see column 6 of Table I). Further, lesser values for  $B(0)$  would yield even higher values for  $\mu_{\text{tot}}$  and thus does not influence the main conclusions of this paper.

For low Fe concentration alloys the observed weak local susceptibility of Rh can be viewed as all Rh being nearly nonmagnetic. However, considering the LSD calculated results presented in Table I we feel that Rh atoms possess a sizable magnetic moment even for low Fe compositions. Further, from the oscillatory character of the Rh magnetic moment seen from our LSD calculation we conclude that the slight deviation of the local susceptibility  $\beta$  above 1 for  $x \leq 0.03$  (see Fig. 2) arises mainly from individual Rh magnetic atoms contributing different  $B_{\text{hf}}$  values, both positive and negative, adding to produce a very small positive  $\beta(T) - 1$ . Adopting a binomial expansion in the Fe concentration  $x$  for the arrangement of Fe neighbors out to the  $2\text{nn}$  shell around a Rh probe atom, one finds that the majority of such configurations (83% for  $x = 0.01$  and 58% for  $x = 0.03$ ) has no Fe neighbors and is nonmagnetic, but the remainder magnetic Rh atoms add up to an average Curie constant  $\bar{C}$  in the range of  $0-5$  K and hence a  $\beta$  value only slightly greater than one.

Next we discuss the low-temperature magnetic behavior of Rh in the RSG alloy  $\text{Au}_{0.82}\text{Fe}_{0.18}$ . The hyperfine field  $B_{\text{hf}}$  at Rh rises rapidly below the ferromagnetic ordering temperature  $T_c \sim 180$  K and saturates to a value of  $-21$  kG at 60 K. On cooling further, the hyperfine field increases steeply below 60 K identify-

ing the transition to the RSG state seen from Mössbauer and ac magnetization studies.<sup>11,22</sup> The observed temperature dependence of  $B_{\text{hf}}$  at Rh is similar to the behavior of hyperfine fields at  $^{57}\text{Fe}$ ,  $^{119}\text{Sn}$ , and  $^{197}\text{Au}$  in the Au-Fe system.<sup>11</sup> Such a behavior has been interpreted in terms of the so-called spin canting model based on the theoretical work by Gabay and Toulouse<sup>26</sup> in which only the longitudinal spin component  $S_L$  of the local Fe moments order ferromagnetically at  $T_c$ . Below  $T_g$ , the spin-freezing temperature, additional ordering of the transverse components  $S_T$  take place. When studied by local techniques, such as Mössbauer spectroscopy and TDPAC, the hyperfine field, which scales with the total spin  $S$  of the magnetic ion, shows as an enhancement in the  $B_{\text{hf}}$  value. In the RSG state our Rh  $B_{\text{hf}}$  value when extrapolated to zero temperature comes out to be  $-27$  kG (see Fig. 4) which is an enhancement of 1.3 over the corresponding value in the ferromagnetic region. It is interesting to note that the ratio of  $B_{\text{hf}}(0)$  in the RSG and the ferromagnetic region observed from our data is close to the value obtained from  $^{57}\text{Fe}$ ,  $^{119}\text{Sn}$ , and  $^{197}\text{Au}$  Mössbauer studies.<sup>11</sup> Assuming that the magnetic moment at Rh, seen from our paramagnetic local susceptibility data, does not change significantly in the RSG state, the observed increment in the  $B_{\text{hf}}$  value of Rh is consistent with an increase in the total magnetic moment of the surrounding Fe atoms as suggested from the mean-field theory of Gabay and Toulouse.<sup>26</sup>

In summary, we have studied the magnetic behavior of isolated  $^{100}\text{Rh}$  impurities in some  $\text{Au}_{1-x}\text{Fe}_x$  alloys,  $x \leq 0.18$ , in the paramagnetic state, and the RSG phase of  $\text{Au}_{0.82}\text{Fe}_{0.18}$ . The measured local susceptibility at Rh suggests a large magnetic moment at Rh for  $x \geq 0.1$  which is supported from our local spin-density calculations. Our calculations show considerable  $d$ -spin polarization at Rh, both positive and negative when surrounded by one or more Fe atoms in different neighboring atomic coordination shells. The measured temperature dependence of the hyperfine field at Rh in the RSG state of the  $x = 0.18$  alloy shows substantial enhancement below the spin-freezing temperature  $T_g \sim 60$  K which corresponds to an increment of the total spin by 1.3 over its value in the ferromagnetic region and thus provide additional support to the spin-canting model proposed by Gabay and Toulouse.

#### ACKNOWLEDGMENTS

We thank Dr. R. G. Pillay and Dr. P. L. Paulose for valuable discussions. We also thank S. Radha for providing some of the samples. We acknowledge the Pelletron accelerator staff for their cooperation during the experiment.

<sup>1</sup>For a review, see D. Riegel and K. D. Gross, *Physica B* **163**, 678 (1990); K. D. Gross, D. Riegel, and R. Zeller, *Phys. Rev. Lett.* **65**, 3044 (1990).

<sup>2</sup>Olle Eriksson, R. C. Albers, and A. M. Boring, *Phys. Rev. Lett.* **66**, 1350 (1991); Ian Morrison, D. M. Bylander, and L.

Kleinman, *ibid.* **71**, 1083 (1993).

<sup>3</sup>B. V. Reddy, S. N. Khanna, and B. I. Dunlap, *Phys. Rev. Lett.* **70**, 3323 (1993); A. J. Cox, J. G. Louderback, and L. A. Bloomfield, *ibid.* **71**, 923 (1993).

<sup>4</sup>S. Khatua, S. N. Mishra, S. H. Devare, and H.G. Devare, *Phys.*

- Rev. Lett. **68**, 1038 (1992).
- <sup>5</sup>M. R. Press, S. N. Mishra, S. H. Devare, and H. G. Devare, Phys. Rev. B **47**, 14988 (1993).
- <sup>6</sup>V. V. Krishnamurthy, S. N. Mishra, M. R. Press, P. L. Paulose, S. H. Devare, and H. G. Devare, Phys. Rev. B **49**, 6726 (1994).
- <sup>7</sup>K. Willenborg, R. Zeller, and P. H. Dederichs, Europhys. Lett. **18**, 263 (1992).
- <sup>8</sup>D. Riegel, J. Kapoor, A. Metz, and K. D. Gross (unpublished).
- <sup>9</sup>M. J. Zhu, D. M. Bylander, and L. Kleinman, Phys. Rev. Lett. **66**, 1350 (1991).
- <sup>10</sup>S. Khatua, S. N. Mishra, S. H. Devare, and H. G. Devare, Hyperfine Interact. **78**, 553 (1993).
- <sup>11</sup>J. Lauer and W. Keune, Phys. Rev. Lett. **48**, 1850 (1982); S. Lange, M. M. Abd-Elmeguid, and H. Micklitz, Phys. Rev. B **41**, 6907 (1990).
- <sup>12</sup>C. Meyer, F. Hartmann-Bourtron, J. M. Greneche, and F. Varret, J. Phys. (Paris) Colloq. **49**, C8-1155 (1988).
- <sup>13</sup>M. M. Abd-Elmeguid, H. Micklitz, R. A. Brand, and W. Keune, Phys. Rev. B **33**, 7833 (1986).
- <sup>14</sup>M. Rots, L. Hermans, and J. van Cauteren, Phys. Rev. B **30**, 3666 (1984).
- <sup>15</sup>H. E. Mahnke, Hyperfine Interact. **49**, 77 (1989); D. Riegel and K. D. Gross, in *Nuclear Physics Applications in Material Science*, Vol. E144 of NATO Advanced Studies Institute, Series B: Physics, edited by E. Recknagel and J. C. Soares (Plenum, New York, 1988), p. 327.
- <sup>16</sup>D. E. Ellis and G. S. Painter, Phys. Rev. B **2**, 2887 (1970); E. J. Baerends, D. E. Ellis, and P. Ros, Chem. Phys. **2**, 41 (1973).
- <sup>17</sup>P. Hohenberg and W. Kohn, Phys. Rev. B **136**, 864 (1964); W. Kohn and L. J. Sham, Phys. Rev. A **140**, 1143 (1965).
- <sup>18</sup>U. von Barth and L. Hedin, J. Phys. C **5**, 1629 (1972).
- <sup>19</sup>S. Blügel, H. Akai, R. Zeller, and P. H. Dederichs, Phys. Rev. B **35**, 3271 (1987).
- <sup>20</sup>P. Weinberger, J. Banhart, G. H. Schadler, A. M. Boring, and P. S. Riseborough, Phys. Rev. B **41**, 9444 (1990).
- <sup>21</sup>P. Terzieff and E. Wachtel, J. Mater. Sci. **27**, 3359 (1992).
- <sup>22</sup>B. V. B. Sarkissian, J. Phys. F **11**, 2191 (1981); U. Larsen, Phys. Rev. B **18**, 5014 (1978); Solid State Commun. **22**, 311 (1977).
- <sup>23</sup>J. G. Perez-Ramirez and P. Steiner, J. Phys. F **7**, 1573 (1977); T. A. Kitchen and R. D. Taylor, Phys. Rev. B **9**, 344 (1974).
- <sup>24</sup>A. Metz, K. D. Gross, W. D. Brewer, and D. Riegel (unpublished).
- <sup>25</sup>R. E. Watson and A. J. Freeman, in *Hyperfine Interactions*, edited by A. J. Freeman and R. B. Frankel (Academic, New York, 1967), p. 53.
- <sup>26</sup>M. Gabay and G. Toulouse, Phys. Rev. Lett. **47**, 201 (1981).
- <sup>27</sup>*Metallic Shifts in NMR*, Progress in Material Science Vol. 20, Part I, edited by D. C. Carter, L. H. Bennett, and D. J. Kahan (Pergamon, New York, 1977), p. 1.
- <sup>28</sup>H. Akai, M. Akai, S. Blügel, B. Drittler, H. Ebert, K. Terakura, R. Zeller, and P. H. Dederichs, Prog. Theor. Phys., Suppl. **101**, 11 (1990).
- <sup>29</sup>G. N. Rao, Hyperfine Interact. **24-26**, 1119 (1985).